Materials Research, Vol. 9, No. 3, 281-286, 2006

Comparison of the Corrosion Resistance of DIN W. Nr. 1.4970 (15%Cr-15%Ni-1.2%Mo-Ti) and ASTM F-138 (17%Cr-13%Ni-2.5%Mo) Austenitic Stainless Steels for Biomedical Applications

Maysa Terada[a], Renato Altobelli Antunes[b], Angelo Fernando Padilha[b], Hercílio Gomes de Melo[c], Isolda Costa[a]*

[a]*Instituto de Pesquisas Energéticas e Nucleares – IPEN/CNEN-SP, Centro de Ciência e Tecnologia de Materiais – CTM, Av. Professor Lineu Prestes, 2242, Cidade Universitária, 05508-900 São Paulo - SP, Brazil*
[b]*Escola Politécnica da USP, Departamento de Engenharia Metalúrgica e de Materiais, Av. Prof. Mello Moraes, 2463, Cidade Universitária, Butantã, 05508-030 São Paulo - SP*
[c]*Escola Politécnica da USP, Departamento de Engenharia Química, Av. Prof. Luciano Gualberto, Trav. 3, n. 380, 05508-900*

Received: December 7, 2005; Revised: August 22, 2006

The resistance to localised corrosion of the full austenitic 15%Cr-15%Ni-1.2%Mo titanium stabilized stainless steel (DIN W. Nr. 1.4970) was investigated by electrochemical methods including electrochemical impedance spectroscopy (EIS), potentiodynamic polarization and potentiostatic polarization measurements in a phosphate-buffered solution (PBS). The low carbon and non-stabilized austenitic stainless steel, AISI 316L (ASTM F-138), widely used for surgical implants, was also tested for comparison. The tests were conducted at room temperature after a stable potential had been reached. After the electrochemical measurements, the surfaces of the specimens were observed using SEM to evaluate the presence of pits. Potentiodynamic polarization results showed that both steels are prone to localized corrosion. Larger pits were found on the surface of AISI 316L specimens after the electrochemical tests. EIS response has indicated the duplex structure of the passive oxides. The results showed that the electrochemical behaviour of the DIN W. Nr. 1.4970 is better than of AISI 316L steel. Therefore, their application as an implant material may be considered.

Keywords: *corrosion, austenitic stainless steel, surgical implants*

1. Introduction

Metallic implants must present a favourable combination of properties such as Young's modulus or modulus of elasticity, yield strength, ductility, toughness, and corrosion resistance. Titanium alloys are widely used as biomaterials due to their mechanical and corrosion properties. However, these alloys are considerably expensive for applications as orthopaedic materials, mainly for the poor population, suggesting that cheaper materials with similar properties should be tested to substitute them. In recent years, prosthesis made of stainless steels have been widely used in public services[1]. Austenitic stainless steels (SS) are the main class of materials when the cost is of major importance for the selection of the material for application as implants. The ASTM F-138 SS is the main material for such use. Its corrosion resistance is moderately good, although comparatively lower than that of titanium alloys.

Milosev and Strehblow[2] have studied the corrosion behaviour of SS in a physiological solution and concluded that the presence of chromium and molybdenum in the passive layer, associated with the depletion of iron in the metallic surface under the passive layer account for the corrosion resistance of orthopaedic implants made of these materials. Many works in the literature report on the electrochemical behaviour of ASTM F-138 in physiological solutions[3-5]. Its susceptibility to localized attack, due to the salts present in these solutions, is commonly reported[6-8].The contact of corrosion products with surrounding tissues may lead to adverse reactions, such as infectious or allergenic responses which, in turn, may cause premature implant failure. Despite these problems, stainless steel implants are still currently used due to a combination of corrosion resistance, mechanical strength, ductility, toughness and easy fabrication at low cost.

Among the SS, the ASTM F-138 has been widely used for biomedical applications, including both temporary and permanent implants. It is an austenitic stainless, low carbon, unstabilized surgical steel grade. Delta-ferrite, strain induced martensites and intermetallic phases such as sigma, chi and Laves phases can be present in the microstructure of the most unstabilized and stabilized austenitic stainless steels such as AISI 316, AISI 316L, AISI 321 and AISI 347[9,10]. The presence of the ferromagnetic phases, delta-ferrite or strain induced martensite, in austenitic stainless steel implants is known to produce adverse interactions between magnetic fields and the implant material. These interactions may lead to magnetic resonance if the patient undergoes a magnetic resonance imaging (MRI) test[11].

The austenitic SS DIN W. Nr. 1.4970 (15%Cr-15%Ni-1.2%Mo-Ti-B) does not form any ferromagnetic phases, like delta-ferrite or martensite, or intermetallic phases, such as sigma, chi and Laves phase, due to its relatively low Cr/Ni ratio and well-adjusted molybdenum and titanium contents[12-14]. Due to this property, it can be considered as a potential material for biomedical applications. The austenitic stainless steel DIN W. Nr. 1.4970 was originally developed for use as core in the nuclear sodium-cooled fast reactor. Its recommendation was based on the superior creep resistance at high temperatures[15]. On the other hand, the room temperature mechanical properties, such as

*e-mail: maysaterada@uol.com.br

Young modulus, yield strength, ductility and toughness of the steels ASTM F-138 and DIN W. Nr. 1.4970 are very similar. However, the corrosion resistance of this latter steel has not yet been investigated with the purpose of use as biomaterial.

The aim of this work was to characterize the localized corrosion resistance of DIN W. Nr. 1.4790 SS in PBS solution at room temperature. EIS, cyclic potentiodynamic polarization and potentiostatic polarization were used as investigation techniques. For comparison, the reference material ASTM F-138 SS was investigated in the same manner. The pits morphology after the electrochemical measurements was observed using scanning electron microscopy (SEM).

2. Experimental

The chemical compositions of the materials are shown in Table 1. All specimens were ground up to #600 with silicon carbide paper, and then cleaned with deionized water, degreased with acetone and immersed in a phosphate-buffered solution (PBS) at room temperature for 24 hours prior to the electrochemical measurements. The composition of the PBS solution is given in Table 2.

Both steels were tested after solution annealing heat treatment. The presence and amount of precipitates in the steel DIN W. Nr. 1.4970 after solution annealing was evaluated by a phase separation technique that comprised selective dissolution of the matrix in a Berzelius type solution, filtering and weighing of the precipitates, and finally their analysis by X ray diffraction using a Guinier-Jagodzinski camera. A detailed description of the microstructural analysis procedures has been published elsewhere[11-13]. The determination of eventual ferromagnetic phases was done on a Fisher ferritoscope. The equipment has a 0.1% ferrite detection limit.

The corrosion tests were performed using a three-cell set-up, with a platinum wire and a saturated calomel electrode (SCE) as counter and reference electrodes, respectively. EIS measurements were accomplished with a 1255 Solartron frequency response analyser coupled to an EG&G 273A potentiostat. All EIS measurements were performed in potentiostatic mode at the open-circuit potential (OCP). The amplitude of the perturbation signal was 10 mV and the investigated frequency range was from 100 kHz to 10 mHz with an acquisition rate of 6 points per decade.

All polarization measurements were taken started after the EIS tests. Potentiodynamic polarization curves were obtained in the range from - 800 mVSCE up to 1200 mV vs OCP with a scan rate of 1 mV s^{-1}. From these curves the pitting potential, the corrosion current density, the corrosion potential and the passive current density were obtained. Potentiostatic polarization tests were also performed at various potentials, with 50 mV increments, starting from 50 mV below the pitting potential, which was determined from the potentiodynamic polarization curves. The potential was maintained during 30 minutes while the corrosion current density was monitored. The breakdown potentials for the two SS were determined from the potentiostatic tests, corresponding to the potential at which the current increased with time.

The pits morphology after polarization was observed using a scanning electron microscope Philips XL30.

3. Results and Discussion

Ferromagnetic phases were not detected and the microstructures of both steels were fully austenitic after solution annealing. Minor amounts (about 0.4 total weight-%) of three types of titanium bearing precipitates were identified in the DIN W. Nr. 1.4970 steel: (Ti,Mo)C, Ti(N,C) and $Ti_4C_2S_2$ (see Table 3). The average diameter of the precipitates was about 5 μm. While the carbides and sulphides were round, slightly elongated, the nitrides were facetted and roughly parallelepipedal. Moreover, the precipitates were found intragranularly and at grain boundaries. On the other hand, in the ASTM F-138 SS microstructure, only few non-metallic inclusions were found.

Figure 1 shows the OCP versus time curves of DIN 1.4970 and ASTM F-138 SS in PBS solution at 25 °C. For the former steel the potential readily stabilizes, and presents small oscillations around a mean value of - 20 mV/SCE. Conversely, the OCP of ASTM F-138 increased steadily during a long period, indicating oxide layer thickening, and stabilized at a value around 0 mV/SCE after 20 hours of test. These results point towards a better stability of DIN 1.4970 in the test solution, which is a desirable property for the use of the material as implant.

EIS diagrams obtained after 24 hours of immersion in the test solution at room temperature are shown in Figure 2 as Bode (phase angle) and Nyquist plots for ASTM F-138 and DIN W. Nr. 1.4970 SS. Both samples presented highly capacitive behaviour in the investigated frequency range, with phase angles close to - 80°, and high impedances, indicating that the oxide layer affords good corrosion protection to the underlying metal. Both phase angle diagrams are depressed in the lower frequency region indicating that they are

Table 1. Chemical compositions of ASTM F-138 and DIN W. Nr. 1.4970 stainless steels.

Steel	C	Cr	Ni	Mo	Si	Mn	Others	Fe
F-138	0.007	17.40	13.50	2.12	0.37	1.78	-	Balance
1.4970	0.09	14.60	15.00	1.25	0.46	1.70	Ti = 0.46	Balance

Table 2. Composition of the PBS solution.

NaCl	8.77 g/L
Na_2HPO_4	1.42 g/L
KH_2PO_4	2.72 g/L
pH	7

Table 3. Crystal structures and lattice parameters of the primary precipitates identified in the steel DIN W. Nr. 1.4970 after solution annealing.

Phase	Crystal structure	Lattice parameter, nm
(Ti,Mo)C	fcc	a = 0.43232
Ti(N,C)	fcc	a = 0.42517
$Ti_4C_2S_2$	hcp	a = 0.32046; c = 1.12086

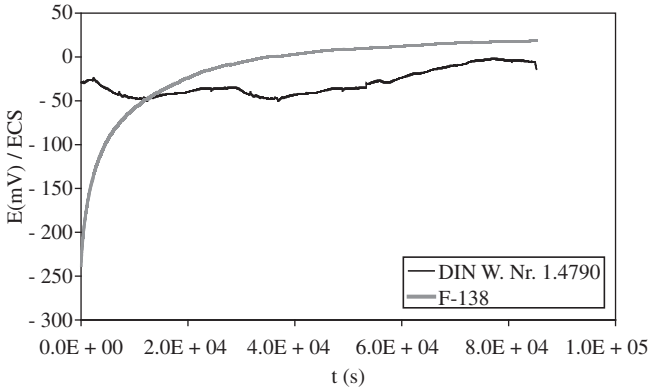

Figure 1. OCP variation for AISI 316L (ASTM F-138) and DIN W. Nr. 1.4970 SS in PBS solution at room temperature.

not composed by a single time constant. Moreover, the capacitive response for DIN W. Nr. 1.4970 starts at higher frequencies, indicating a better response of the oxide layer. Several equivalent circuits proposed in the literature to fit experimental data for SS[16,17] were tested in this investigation, including the simplest one composed only of the R//CPE association in series with the electrolyte resistance. The fitting quality to this latter equivalent circuit was very poor, leading us to employ more complex schemes. The best results were obtained with the equivalent circuit shown in Figure 3[16,17] Table 4 presents the values of the parameters obtained from the fitting procedure. CPEs were used instead of the capacitances in order to take into consideration surface heterogeneities.

An analysis of the capacity values in Table 4 shows that they are two orders of magnitude lower than those normally attributed to the double layer capacity, which lies between 10 and 100 μF.cm^2; however they are both of the same order of magnitude as those associated with thin oxide layers with thicknesses in the range of tenths of nanometers. Accordingly, due to the very low corrosion currents exhibited by both materials at the OCP (*cf*. Figure 4) it is unlikely that any corrosion reaction taking place at the metal interface would be detected by the experiments, and the impedance response can be completely attributed to the oxide layer. It has been proposed in the literature[16,17] that the oxide layer formed on the surface of SS has a duplex structure. The inner layer is composed mainly of chromium oxides and has properties typical of p-type semiconductors, whereas the outer layer, formed by iron oxides and hydroxides, presents n-type semiconductors properties. The results of the fitting procedure indicate that impedance measurements can detect such duplex structure. In this fashion, in the proposed equivalent circuit, the pair R_1//CPE_1 is associated with the outer layer, whereas R_2//CPE_2 can be ascribed to the inner layer. Quantitative analyses of the data show that for both steels, as expected, the corrosion resistance is mainly afforded by the chromium-rich inner layer; however, the layers resistances associated with DIN 1.4970 SS are more than twice higher than those obtained for the AISI 316L, pointing towards a better corrosion resistance of the former. The high-quality of the fitting procedure is also indicated in Figure 2. In addition, the chi-squared values (χ^2) obtained were very low (in the order of 10^{-3}) providing further evidence of the good adjustment.

Potentiodynamic polarization curves for both steels in PBS solution are shown in Figure 4. In accordance with the impedance measurements, they show higher corrosion current densities for the ASTM F-138 SS than for the DIN W. Nr. 1.4970. In addition, a higher pitting potential was associated with this latter type of steel. Very low

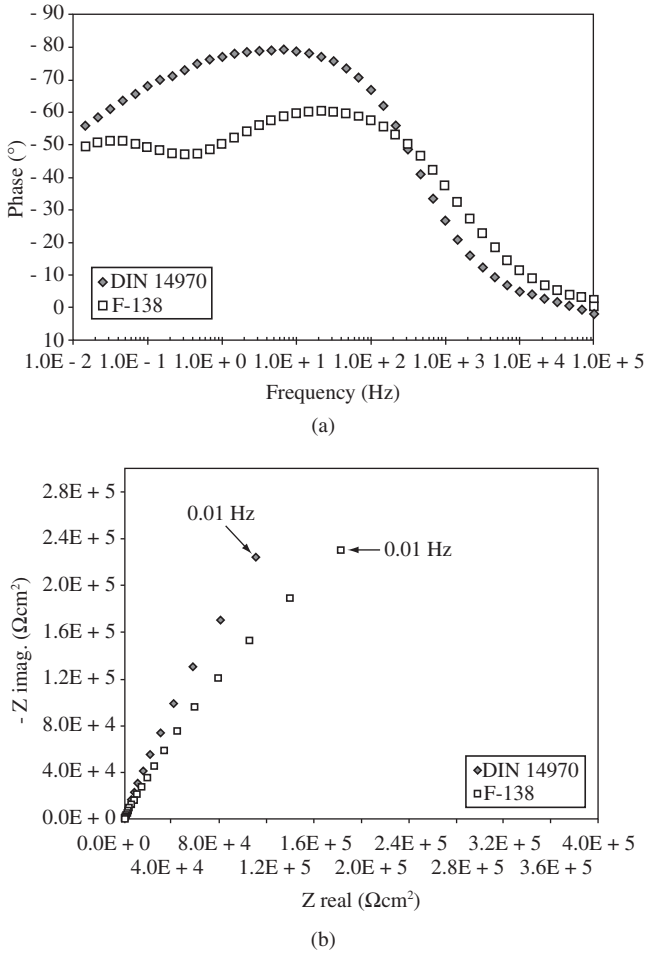

Figure 2. EIS diagrams as a) Bode (phase angle); b) Nyquist plots for ASTM F-138 and DIN W. Nr. 1.4970 in PBS solution at room temperature.

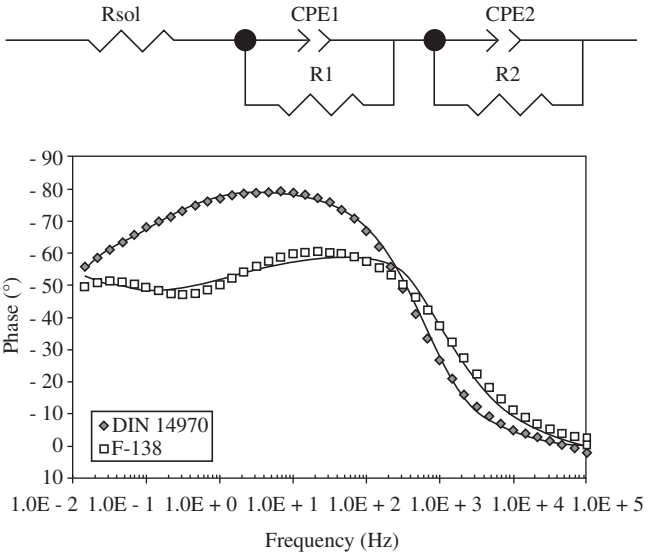

Figure 3. Equivalent circuit used to fit the impedance data for ASTM F-138 and DIN W. Nr. 1.4970 in PBS solution at room temperature.

Table 4. Results of the parameters obtained from the fitting of the equivalent circuit for the experimental data obtained for AISI 316L (ASTM F-138) and DIN W. Nr. 1.4970 SS in PBS solution at room temperature.

Alloy	R_s (Ω.cm^2)	CPE_1 (μFcm^{-2})	R_1 (Ω.cm^2)	CPE_2 (μFcm^{-2})	R_2 (MΩ.cm^2)	Chi-squared
AISI 316 L (F-138)	60.62	0.356	9485	0.568	0.416	0.00416
DIN 1.4970	43.28	0.573	26134	0.242	0.856	0.00198

corrosion current densities (order of 10^{-6} A.cm^{-2}), typical of passive metals, were obtained for both steels at the corrosion potential. Both steels showed susceptibility to pitting corrosion but surface observation, after potentiodynamic polarization tests, revealed much larger and deeper pits on the ASTM F-138 SS comparatively to the DIN W. Nr. 1.4970.

Potentiostatic polarization curves obtained just below the breakdown potentials determined from Figure 4 for the ASTM F-138 and DIN W. Nr. 1.4970 are shown in Figure 5. These breakdown potentials were approximately E = 400 mV/SCE and E = 1000 mV/SCE for the former and the latter steel, respectively.

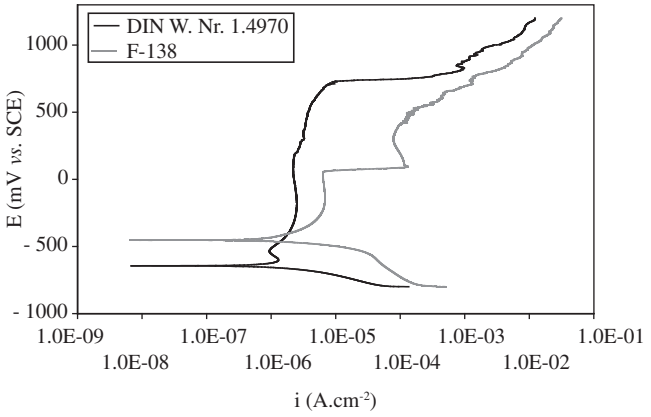

Figure 4. Potentiodynamic polarization curves for ASTM F-138 and DIN W. Nr. 1.4970 stainless steels in PBS solution at room temperature.

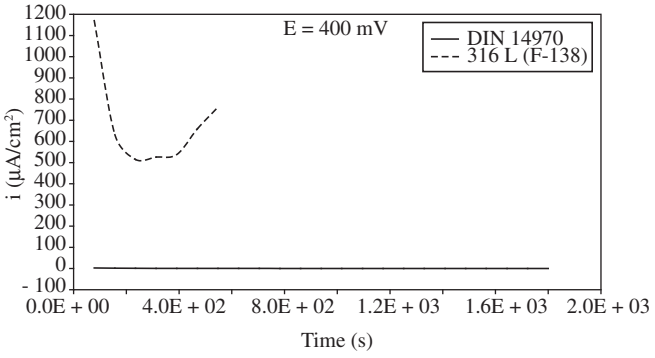

(a)

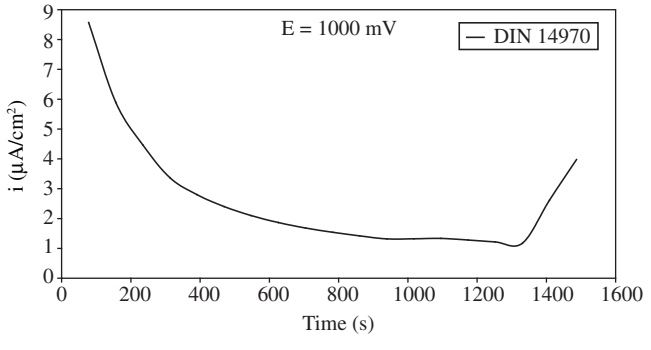

(b)

Figure 5. Potentiostatic polarization curves for ASTM F-138 and DIN W. Nr. 1.4970 stainless steels a) E = 400mV; and b) E = 1000 mV.

The main feature evidenced in the potentiostatic curves presented in Figure 5 for ASTM F-138 and DIN W. Nr. 1.4970 steels, besides the larger difference in breakdown potentials, is the higher anodic current densities through the oxide film on the former SS. This behaviour confirms the previous results, which indicated a more stable and protective oxide layer on the surface of DIN W. Nr. 1.4970 SS. Moreover, the results presented in Figure 5 show that near to their respective breakdown potentials, the induction time for stable pitting growth is much higher for the DIN W. Nr. 1.4970 SS when compared with the other tested steel.

Although electrochemical results have presented a large variability, with some specimens showing a strong tendency to pitting and others high pitting resistance, for most specimens tested, the oxide layer on the DIN W. Nr. 1.4970 was indeed more protective than on the ASTM F-138 SS. Undoubtedly, it was clearly evidenced by the experimental results that both steels are prone to localized attack when exposed to physiological solution, but the pitting susceptibility of DIN W. Nr. 1.4970 is much lower. Therefore, it can be said that under the harsh conditions normally encountered in biomedical applications there are risks of pitting corrosion for an implant device made out from any of these two materials; however the results of the electrochemical tests have pointed that they are less in the DIN W. Nr. 1.4970 steel.

SEM images of ASTM F-138 and DIN W. Nr. 1.4970 specimens after potentiodynamic polarization tests in PBS solution at room temperature are shown in Figure 6. The susceptibility to localized attack of both materials was confirmed by the SEM micrographs. Pits are present on the surfaces of both steels. However, the pits on the ASTM F-138 are deeper and much larger than those found on the DIN W. Nr. 1.4970, showing that localized attack is more severe for the former SS. These findings support the electrochemical results obtained by EIS and polarization data that indicated a more protective oxide layer on the DIN W. Nr. 1.4970 surface.

If one considers the composition of the steels, the ASTM F-138 SS presents higher chromium and molybdenum contents than DIN W. Nr. 1.4970 (see Table 1). These elements account for the corrosion resistance of stainless steels[15,18-20]. On the other hand, the higher nickel content in the composition of DIN W. Nr.1.4970 must have been related to its improved electrochemical behaviour. Surface investigation techniques such as X ray photoelectron spectroscopy are desirable to explain the corrosion behaviour of this steel and must be considered for future research. Taking only corrosion resistance into account the DIN W. Nr. 1.4970 SS is a potential candidate for use as biomaterial. However, further investigations are required to evaluate the biocompatibility of this steel.

4. Conclusions

The corrosion resistance of the DIN W. Nr. 1.4970 SS to localized corrosion is better than the ASTM F-138, as it was indicated by EIS, potentiodynamic polarization and potentiostatic polarization results. Both steels are prone to localized attack but shallower pits are formed on the DIN W. Nr. 1.4970 SS. The results of corrosion resistance indicated that this last steel may be considered for use as biomaterial, once it shows rather improved corrosion properties than ASTM F-138 SS in physiological solution. Indeed, this result outlines its main attractive feature, that is, the total absence of magnetic phases.

Acknowledgments

The authors acknowledge FAPESP, CNPq and CAPES for financial support. Dr. Clarice T. Kunioshi is also acknowledged for the SEM micrographs.

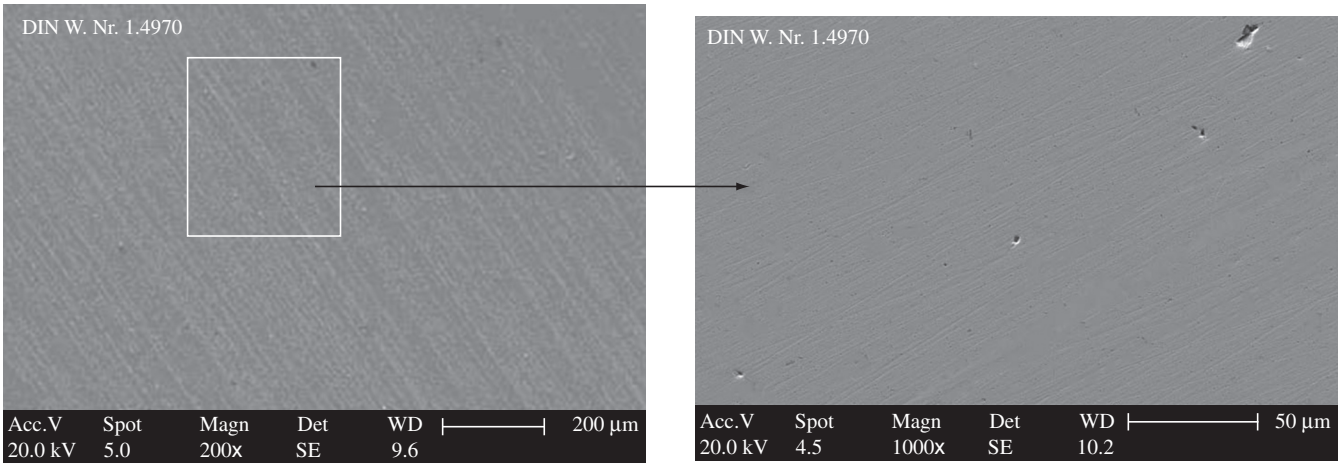

(a)

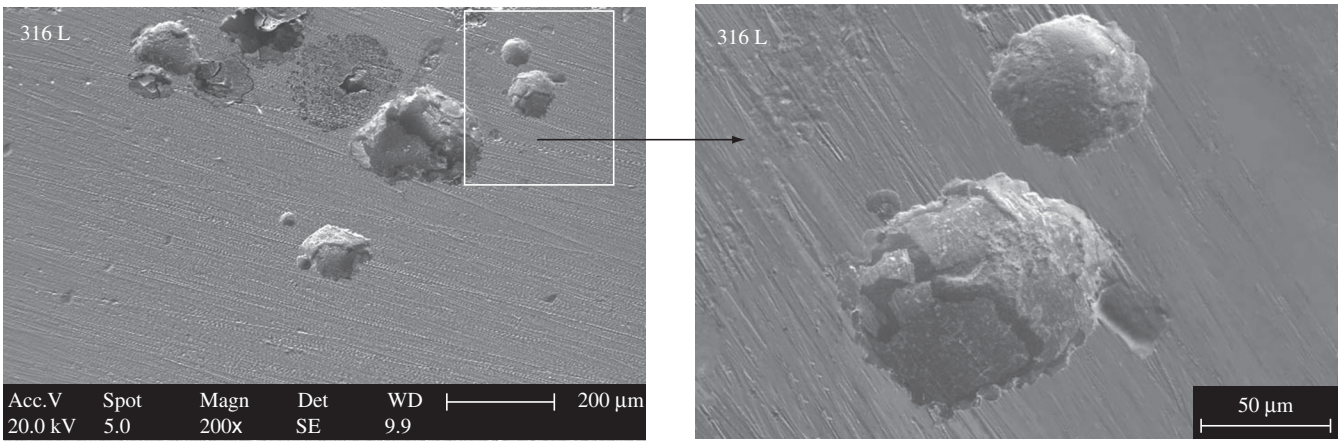

(b)

Figure 6. SEM micrographs of a) DIN W. Nr. 1.4970; and b) ASTM F-138 stainless steels after polarization in phosphate buffered solution.

References

1. Azevedo CRF, Hippert Jr E. Failure analysis of surgical implants in Brazil. *Engineering Failure Analysis*. 2002; 9(6):621-633.
2. Milosev I, Strehblow H-H. Electrochemical behavior of Cu-xZn alloys in borate buffer solution at pH 9.2. *Journal of Biomedical Materials Research*. 2000; 52(2):404-412.
3. Gurappa I. Characterization of different materials for corrosion resistance under simulated body fluid conditions. *Materials Characterization*. 2002; 49(1):73-79.
4. Duisabeau L, Combrade P, Forest B, *Wear*. Amsterdam: Elsevier; 2004.
5. Arumugam TK, Rajeswari S, Subbaiyan M. Electrochemical behaviour of advanced stainless steel implant material in saline physiological solution with calcium and phosphate ions and serum protein. *Transactions of the Indian Institute of Metals*. 1998; 51(5):417-420.
6. Sivakumar M, Rajeswari S. Investigation of failures in stainless steel orthopedic implant devices - pit-induced stress corrosion cracking. *Journal of Materials Science Letters*. 1992; 11(15):1039-1042.
7. Sivakumar M, Mudali UK, Rajeswari S. Investigation of failures in stainless steel orthopedic implant devices - pit-induced stress corrosion cracking. *Journal of Materials Science Letters*. 1995; 14(2):148-151.
8. Xie J, Alpas AT, Northwood DO. A mechanism for the crack initiation of corrosion fatigue of Type 316L stainless steel in Hank's solution. *Materials Characterization*. 2002; 48(4):271-277.
9. Padilha AF, Rios PR. Decomposition of austenite in austenitic stainless steels. *ISIJ International* (*Japan*). 2002; 42(4):135-143.
10. Padilha AF, Plaut RL, Rios PR. Annealing of cold-worked austenitic stainless steels. *ISIJ International* (*Japan*). 2003; 43(2):325-337.
11. Woods TO, Stainless steels for medical and surgical applications In: *ASTM Simposium*, EUA; 2002. p. 82-90.
12. Padilha AF. *Ausscheidungsverhalten des titanstabilisierten austenitischen rostfreien 15%Cr-15%Ni-1,2%Mo-Stahles (DIN 1.4970)*, KfK Report 3151, Karlsruhe: Kernforschungszentrum Karlsruhe; 1981.
13. Padilha AF, Schanz G, Anderko K. Precipitation behaviour of titanium stabilized 15%Cr, 15% Ni,1% Mo-TI-B Austenite steel (DIN W. Nr. 1.4970). *Journal of Nuclear Materials*. 1982; 105(1):77-92.
14. Padilha AF. Efeito de tratamentos térmicos e mecanotérmicos sobre o comportamento em tração e fluência a 600°C de aço inoxidável austenítico estabilizado com titânio. *Metalurgia* – ABM (Brazil), 1993; 39(3):413-418.
15. Lagerberg G, Egnell L. Canning materials for fast reactor fuel rods. *Nuclear Engineering International*. 1970; 15(166):203-207.
16. Azumi K, Ohtsuka T, Sato N. Impedance of iron electrode passivated in borate and phosphate solutions. *Transactions of the Japan Institute of Metals*. 1986; 27(5):382-392.
17. Ge H, Zhou G, Wu W. Passivation Model of 316 stainless steel in simulated cooling water and the effect of sulfide on the passive film. *Applied Surface Science*. 2003; 211(2):321-334.

18. Disegi JA, Eschbach L. Stainless steel in bone surgery. *Injury-International Journal of the Care of the Injured*. 2000; 31(4):S2-S6.
19. Hakiki NE, Belo MC, Simões AMP, Ferreira MGS. Semiconducting properties of passive films formed on stainless steels - Influence of the alloying elements. *Journal of Electrochemical Society*. 1998; 145(11):3821-3829.
20. Ramasubramanian N, Preocanin N, Davidson RD. Analysis of passive films on stainless-steel by cyclic voltammetry and Auger-spectroscopy. *Journal of Electrochemical Society*. 1985; 132(4):793-798.